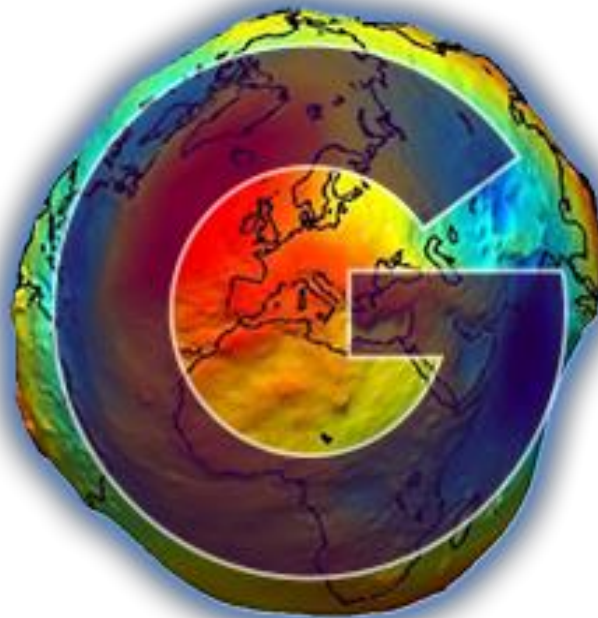


***EO-1-2014: New ideas for Earth-relevant space applications
Research and Innovation action***

Action acronym: **EGSIEM**
Action full title: European Gravity Service for Improved Emergency Management
Grant agreement no: 637010

**Deliverable D4.3
External Validation**

Date: 2017-09-30



Author(s): Qiang Chen, Ulrich Meyer, Lea Poropat



1. Change Record

<u>Name</u>	<u>Author(s)</u>	<u>Date</u>	<u>Document ID</u>
Draft 1	QC, UM, LP	2017-09-13	D4.3_v3
Draft 2	QC, UM, LP	2017-09-21	D4.3_v4
Draft 3			



Table of Contents

1. Change Record	2
2. Overview	4
3. Comparison to official GRACE SDS monthly gravity fields	5
4. Validation based on GNSS loading.....	9
4.1 Validation of EGSIEM Level 2 products	9
4.2 Validation of EGSIEM Level 3 land products	15
5. Validation based on OBP	19
6. Error budgeting	21
7. Bibliography.....	25
8. Glossary.....	26
9. Annexes.....	27

2. Overview

As one of the key scientific services of the EGSiEM project, combined GRACE gravity products are generated using various monthly GRACE solutions from the associated EGSiEM analysis centers (ACs). To ensure the quality of the EGSiEM-generated gravity products, external validation using other independent observations is essential as they can help us to increase user's confidence in the project's data products. This report aims to provide a concise validation of the EGSiEM-generated gravity fields using various external datasets.

According to the EGSiEM proposal, T4.3 aims at validating two-year (2006 and 2007) gravity solutions from T2.3 (individual solutions from ACs) and T4.2 (combined solutions and corresponding Level 3 products) using different external datasets, including:

- 1) comparison with external sources of gravity solutions, e.g. solutions from JPL and CSR
- 2) assessment of gravity solutions using available hydrological models
- 3) validation of gravity solutions using GNSS time series

In this report, validation results of 1) and 3) are presented in Section 3 and Section 4. As the inter-comparison of gravity solutions from 4 ACs and the combined solutions has been intensively documented in D4.2, Section 3 demonstrates only the comparison of the official combined EGSiEM solutions at the NEQ level to the external sources of gravity solutions, i.e. three official gravity solutions from GFZ RL05a, CSR RL05 and JPL RL05.

In Section 4, intensive validation of the EGSiEM Level 2 products as well as Level 3 land grids are implemented using the external GNSS time series. The EGSiEM Level 2 products are validated against the gravity fields from the three official centers, see Section 4.1. The EGSiEM Level 3 land products are validated against the GRACE Tellus Level 3 land products, see Section 4.2.

Due to relatively short time series of the gravity fields, assessment using hydrological models turns out to be not meaningful. Instead, validation using the ocean bottom pressure (OBP) records is conducted and presented in Section 5. However, as only two-year EGSiEM combined data available, no enough OBP records are available to draw strong conclusions from the validation.

Apart from various validations, a short description regarding the error budgeting is also included in Section 6.

3. Comparison to official GRACE SDS monthly gravity fields

For combination of the individual AC's contributions, relative weights are derived by pairwise comparison to the monthly average, iterated by variance component estimation (VCE). This quality criterion is based on the assumption that all considered time-series contain basically the same signal, but differ in noise. For quality control an independent quality criterion has to be defined. We compute monthly residuals of all spherical harmonic coefficients (SHC) to deterministic models of their secular and seasonal (annual and semi-annual) variations, furtheron these residuals are called anomalies. For medium to high degrees and orders the anomalies are expected to represent mainly noise.

For compact visualization degree amplitudes are computed, either to full order, or in an refined analysis to order 29, to reduce the comparison to the geophysically most meaningful part of the spectrum (order 29 was chosen as limit to exclude the second resonance order around 31). Anomalies were computed from the official GRACE SDS time-series CSR-RL05, GFZ-RL05a and JPL-RL05. The reference deterministic model of variations was determined based on the full dataset of available time-series at the International Center for Global Earth Models (ICGEM), excluding only DMT and GRGS due to the regularization applied in the processing.

Evaluated were the two test years of EGSIM 2006 and 2007. Figure 3-1 shows the Median values of the degree amplitudes in equivalent water heights. The EGSIM combined gravity fields clearly show the lowest noise levels.

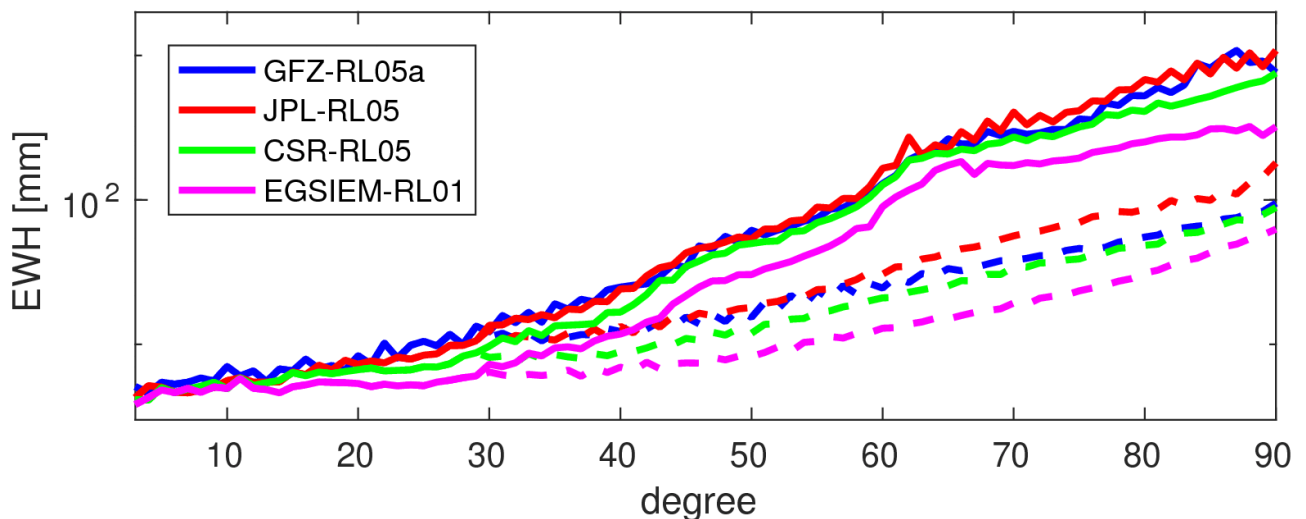


Figure 3-1: Degree amplitudes of anomalies considering all orders (solid lines) or only orders up to 29 (dashed lines).

The SHC anomalies can also be transformed to the spatial domain. Figure 3-2 to Figure 3-5 show the spatial distribution of anomalous signal for the three official GRACE SDS time-series CSR-RL05 (truncated at degree 90), GFZ-RL05a and JPL-RL05, and for the EGSIM combined solutions, in terms of the RMS of anomalies per grid cell (again the years 2006 and 2007 are evaluated). For this purpose the anomalies were smoothed by a 400 km Gauss filter. The geophysically meaningful signal is restricted to the continents, where hydrological events of much shorter than semi-annual period are recorded by the GRACE satellites. With the exception of a small area near the eastern Coast of South America, where rough bathymetry complicates things,

and traces of the Antarctic circumpolar current, the longitudinal striping pattern visible over the oceans can be considered as noise. Again the EGSIM combined solutions clearly outperform the individual GRACE SDS time-series.

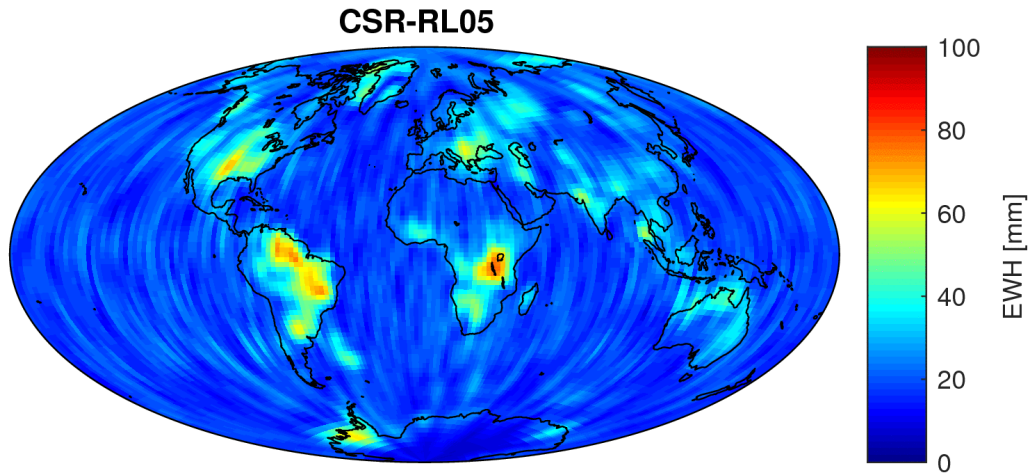


Figure 3-2: RMS of anomalies of GRACE SDS CSR-RL05 gravity fields 2006/2007 (truncated at degree 90).

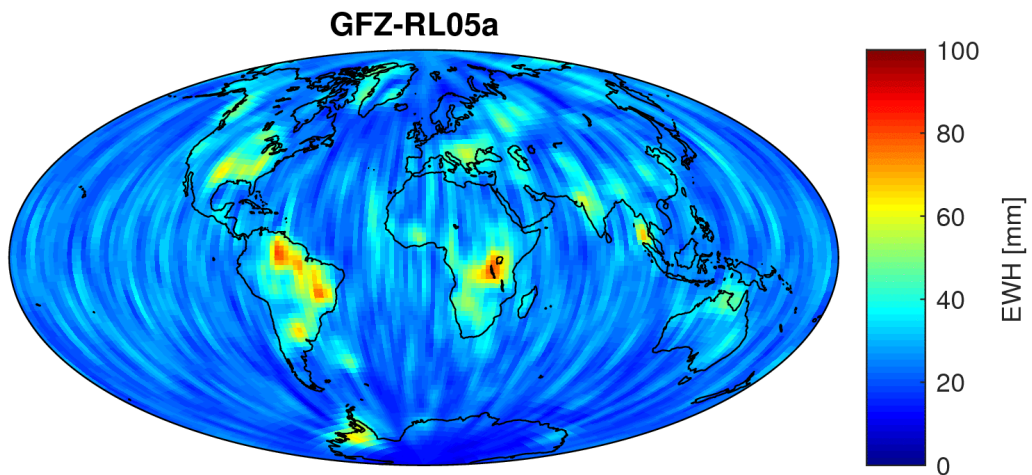


Figure 3-3: RMS of anomalies of GRACE SDS GFZ-RL05a gravity fields 2006/2007.

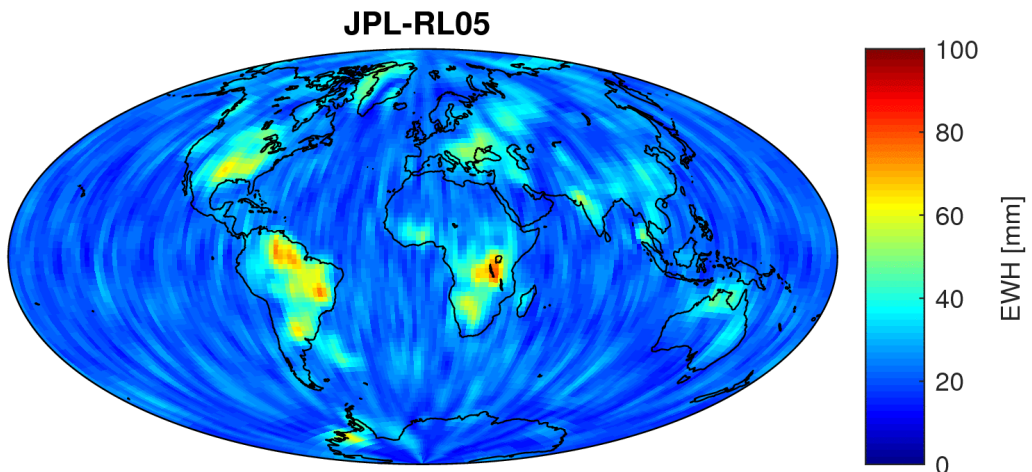


Figure 3-4: RMS of anomalies of GRACE SDS JPL-RL05 gravity fields 2006/2007.

EGSIEM-RL01

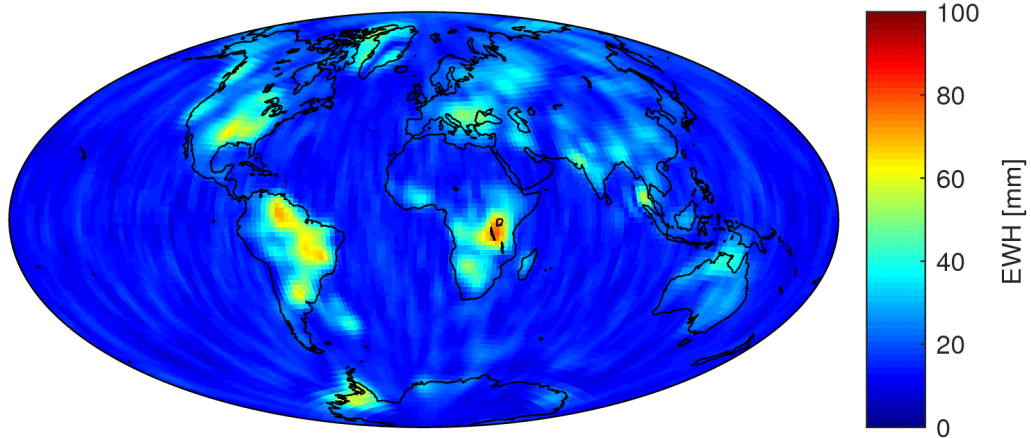


Figure 3-5: RMS of anomalies of combined EGSIM gravity fields 2006/2007.

The anomalies within the ocean regions can be condensed to one number per month, namely the RMS over all ocean grid cells. The ocean grid cells are weighted by the cosine of the latitude of their mid points to account for their different sizes. Moreover a small margin around the continents is not taken into account to avoid any leakage of signal from the continents. In our case the original gravity fields in spherical harmonic representation up to degree and order 90 were transformed into the corresponding global grids of 2 degree cell size and a margin of three cells, i.e., 6 degrees along all coast lines, were removed when computing the weighted RMS per month over the oceans. The corresponding monthly RMS values for the different time-series of gravity fields are given in Figure 3-6 (no smoothing applied) and Figure 3-7 (with 400 km Gauss filter, corresponding to Figure 3-2 to Figure 3-5). In both cases the generally lower noise of the combined EGSIM solutions is clearly visible.

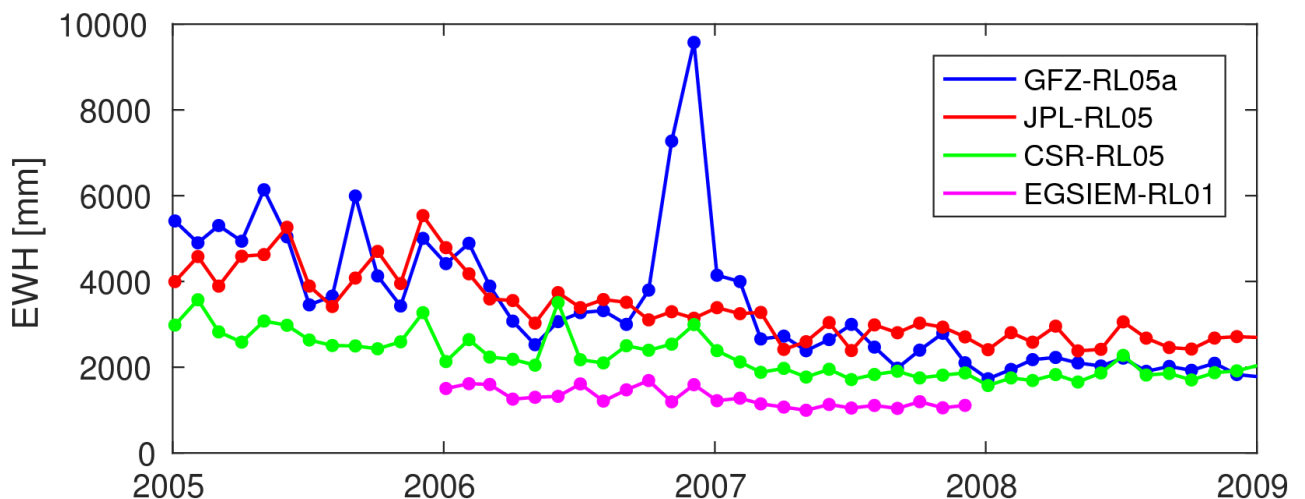


Figure 3-6: Monthly weighted RMS of unfiltered anomalies over the oceans (CSR-RL05 truncated at degree 90).

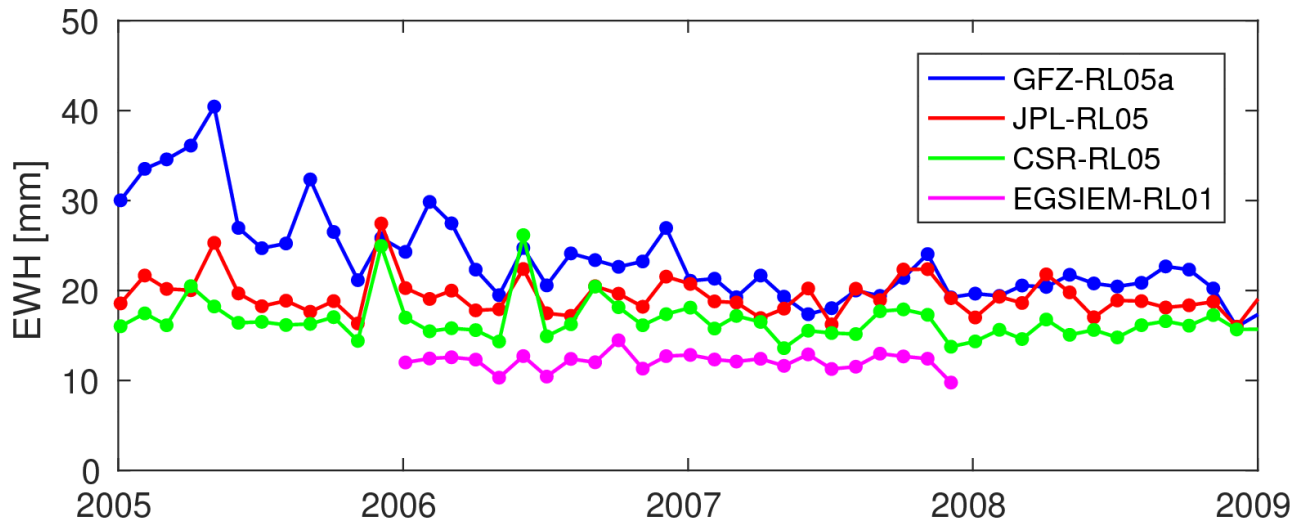


Figure 3-7: Monthly weighted RMS of anomalies over the oceans smoothed by a 400 km Gauss filter (CSR-RL05 truncated at degree 90).

We conclude that in term of noise the EGSIM combined solutions clearly outperform all official GRACE SDS time-series of monthly gravity fields in SHC. This is true for unfiltered as well as for moderately filtered solutions (tested was a 400 km Gauss filter).

4. Validation based on GNSS loading

The concept of validating the GRACE products using GNSS loading will be explained in detail in D3.2 and therefore it will not be repeated here. We use the external GNSS datasets provided by Rebischung et al. (2016), which are the latest ITRF2014 daily residuals at 1054 GNSS stations globally. These GNSS residuals are free of outliers, offsets and linear trends. To compare with monthly GRACE solutions, these daily solutions are averaged into monthly solutions and 388 GNSS stations with full monthly solutions of 2006 and 2007 are selected. It should be mentioned that only the vertical component of the GNSS time series is used during the whole validation process in Section 4.1 and Section 4.2.

In Section 4.1, we compare the two-year gravity solutions from four analysis centers (ACs) and the combined solutions (both at solution level and NEQ level) against the official GRACE SDS using GNSS loading. In Section 4.2, the EGSIEM-generated Level 3 products for hydrology are validated against the Level 3 grids from GRACE Tellus using the same GNSS data.

To evaluate the performances of different GRACE solutions, we use WRMS reduction (van Dam et al., 2007) and its variants, i.e. degree-dependent WRMS reduction and accumulative degree-dependent WRMS reduction (see Annexes), at the full signal, the annual signal and the residual signal level.

4.1 Validation of EGSIEM Level 2 products

For comparing with the GNSS time series, all the GRACE L2 GSM SHCs from both EGSIEM and SDS have been post-processed in the same way. Firstly, C_{20} term is replaced with that from SLR (Cheng et al. 2011). Degree-1 coefficients are restored using the SLR-derived coefficients provided by UBERN (Sośnica et al. 2015) to be consistent with GNSS in the same reference frame. The EGSIEM combined dealiasing products, i.e. GAC products, have also been restored to GSM SHCs. Finally, all GSM SHCs are filtered with the Gaussian filter with the smoothing radius of 500 km and converted into the vertical displacements at the selected GNSS stations.

At the full signal level

Figure 4-1 presents the mean WRMS reduction at the full signal level for the nine considered gravity solutions. Note that we compute the degree WRMS reduction and accumulative degree WRMS reduction up to the maximum degree of each gravity solutions, i.e. up to full spectrum. However, it is displayed in Figure 4-1 that no significant contributions come from degrees beyond 30. Thus, we show degree statistics up to degree 40 only.

It is clearly depicted that most of the WRMS reduction contributions lie in lower degrees. Degree-1 coefficients from SLR contribute roughly a mean WRMS reduction of 5.42% over 388 GNSS stations. Starting from degree-2, different gravity solutions perform differently, for example, EGSIEM-GRGS shows the best WRMS reduction of 6.38% at degree-2 which is probably due to their constraint of the degree-2 SHCs using the SLR observations. EGSIEM-NEQ provides the second best statistic number of 5.87% at degree-2. All the gravity solutions display negative WRMS reduction at degree-5 and degree-10 which will be assessed further using longer gravity solutions rather than only two years here.

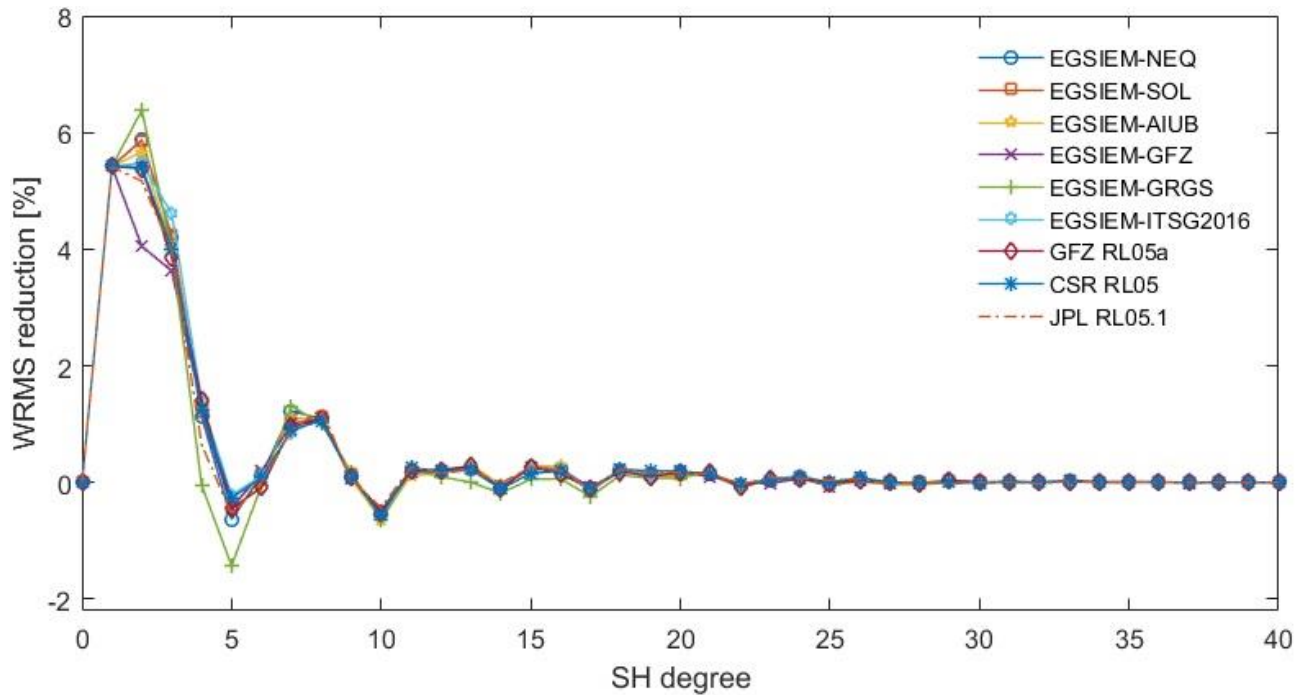


Figure 4-1: Mean degree WRMS reduction of different gravity solutions at the full signal level up to degree 40.

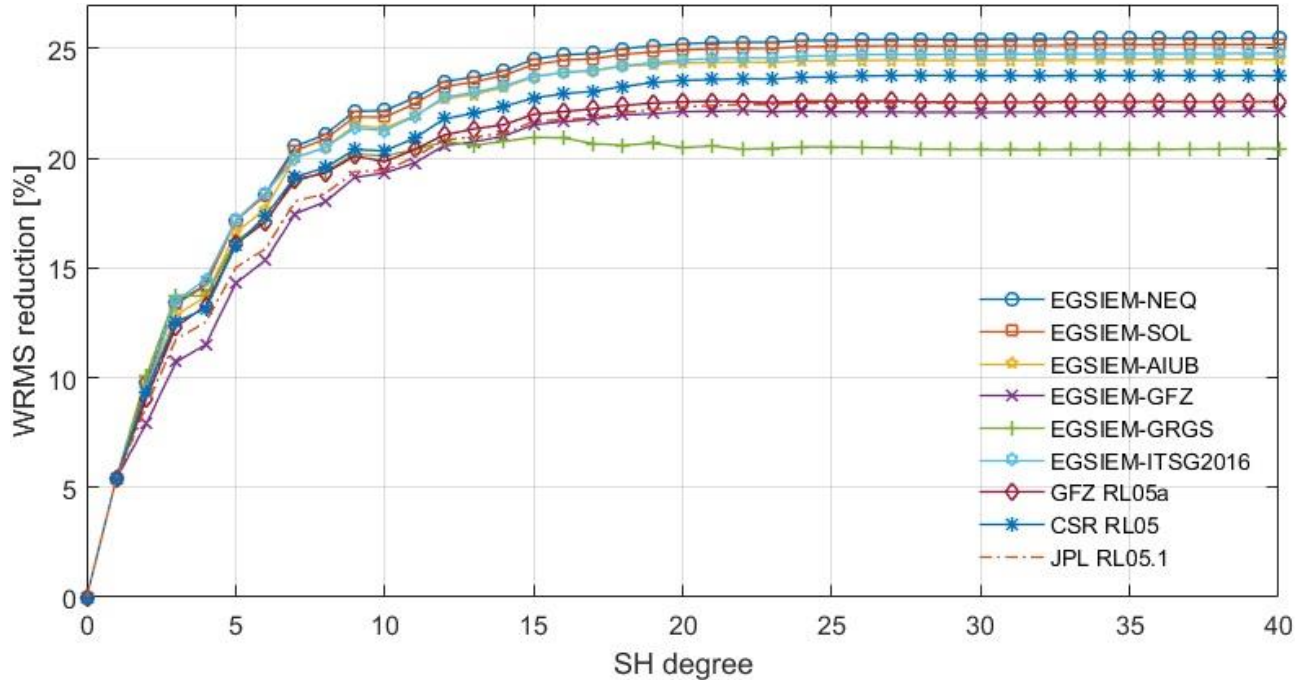


Figure 4-2: Mean accumulative degree WRMS reduction of different solutions at the full signal level up to degree 40.

Figure 4-2 illustrates the mean accumulative degree WRMS reduction over 388 selected GNSS stations for all the GRACE solutions. Both EGSIM combined solutions show the best mean accumulative degree WRMS reductions. EGSIM-NEQ provides a mean of 25.48% WRMS reduction. Note that all the gravity solutions show better mean WRMS reductions compared to the latest results (maximum mean WRMS reduction up to 15%, see Table S3) published by Gu et al (2017) who have done comparisons between GPS and GRACE using multi-institution products. This is probably due to the improved GRACE solutions as well as GNSS datasets we used in our validation process.

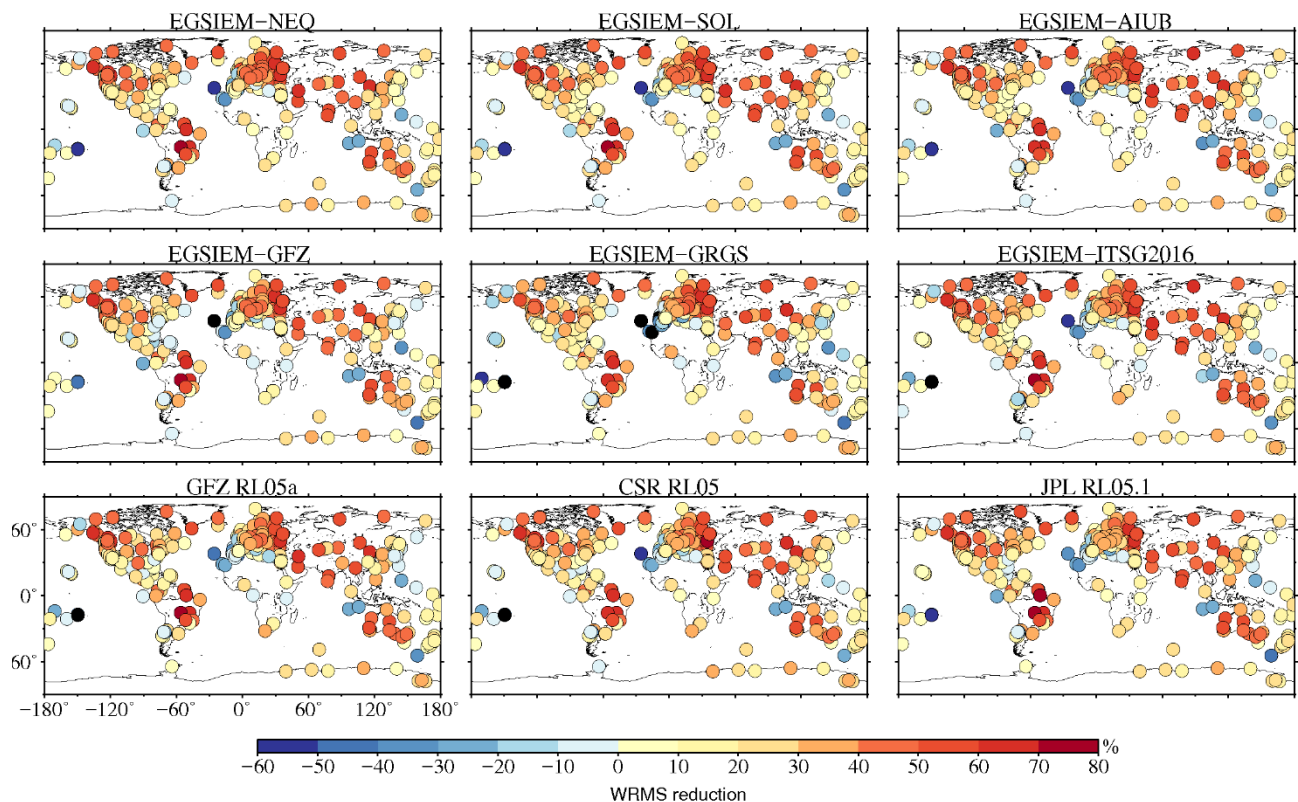


Figure 4-3: WRMS reduction at the full signal level at 388 global GNSS stations. GRACE gravity solutions up to their full spectrum are used to compute the displacements.

The spatial plots of the WRMS reduction from all the gravity solutions up to the full spectrum are shown in Figure 4-3. Up to 70% WRMS reductions are observed for all the gravity solutions at the CUIB station located in Cuiabá, Brazil, where we have strong water mass variations in the Amazon river basin. As seen from the spatial plots in Figure 4-3, most of stations show yellow to red colors, i.e. positive WRMS reductions. The statistics from Figure 4-2 and Figure 4-3 are summarized in Table 4-1. Clearly, EGSIM-NEQ outperforms other gravity solutions with the best mean and positive WRMS reductions with respect to the 388 ITRF2014 GNSS time series.

Table 4-1 Mean and positive WRMS reductions between nine GRACE products and the ITRF2014 residuals at the full signal level.

	Mean WRMS reduction [%]	Positive WRMS reduction [%]
EGSIEM-NEQ	25.48	89.95
EGSIEM-SOL	25.18	89.43
EGSIEM-AIUB	24.50	89.69
EGSIEM-GFZ	22.17	83.51
EGSIEM-GRGS	20.96	81.70
EGSIEM-ITSG2016	24.78	88.66
GFZ RL05a	22.61	84.79
CSR RL05	23.78	88.14
JPL RL05.1	22.56	86.08

At the annual signal level

Besides evaluation at the full signal level, we also look at their performances at the annual signal level. Figure 4-4 and Figure 4-5 display the median degree WRMS reductions and accumulative degree WRMS reductions. The reason to use median here is to avoid the extreme negative WRMS reductions (less than -100%), for example, the black dots shown in Figure 4-6.

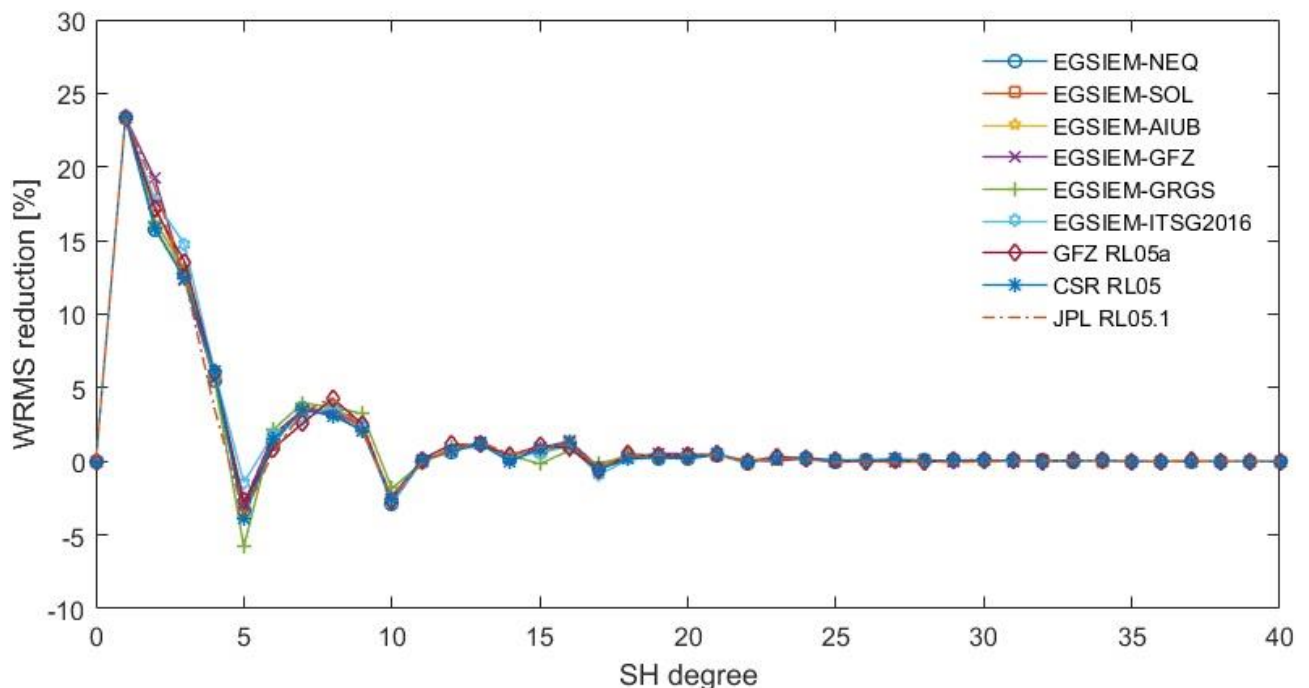


Figure 4-4: Median degree WRMS reduction of different gravity solutions at the annual signal level up to degree 40.

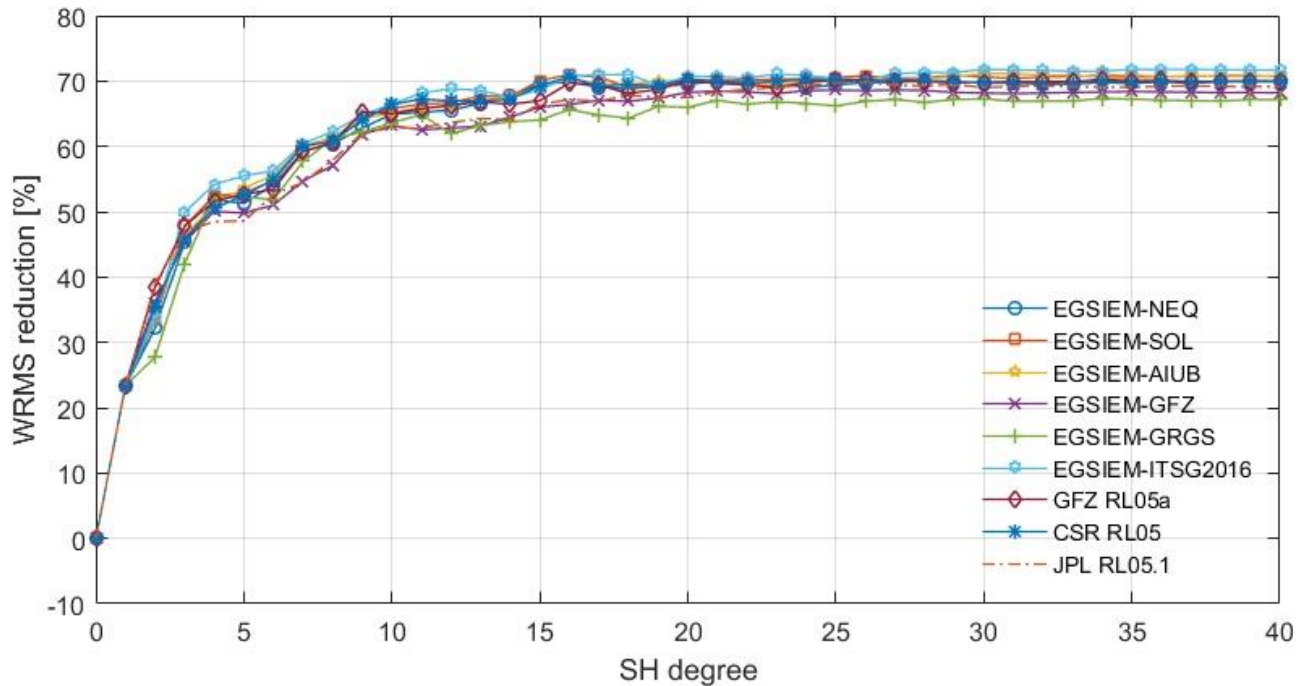


Figure 4-5: Median accumulative degree WRMS reduction of different gravity solutions at the annual signal level up to degree 40.

Similar patterns are found at the annual signal level (Figure 4-4 and Figure 4-5) as shown at the full signal level but with higher WRMS reductions. Up to median values of 70% WRMS reduction are observed for EGSIM-NEQ, EGSIM-SOL, EGSIM-AIUB, EGSIM-ITSG2016, GFZ RL05a and CSR RL05. As shown in Figure 4-6, a bunch of stations show up to 99% agreement between GNSS-observed and GRACE-derived displacements at the annual signal level.

Inspection of the Figure 4-6 as well as Table 4-2, it is demonstrated that all the gravity solutions perform quite similar at annual signal level.

Table 4-2 Median and positive WRMS reductions between nine GRACE products and the ITRF2014 residuals at the annual signal level.

	Median WRMS reduction [%]	Positive WRMS reduction [%]
EGSIEM-NEQ	70.05	88.40
EGSIEM-SOL	70.74	88.14
EGSIEM-AIUB	70.64	88.40
EGSIEM-GFZ	68.28	87.11
EGSIEM-GRGS	67.03	88.40
EGSIEM-ITSG2016	71.63	88.40
GFZ RL05a	70.20	88.40
CSR RL05	70.20	87.89
JPL RL05.1	69.17	87.63

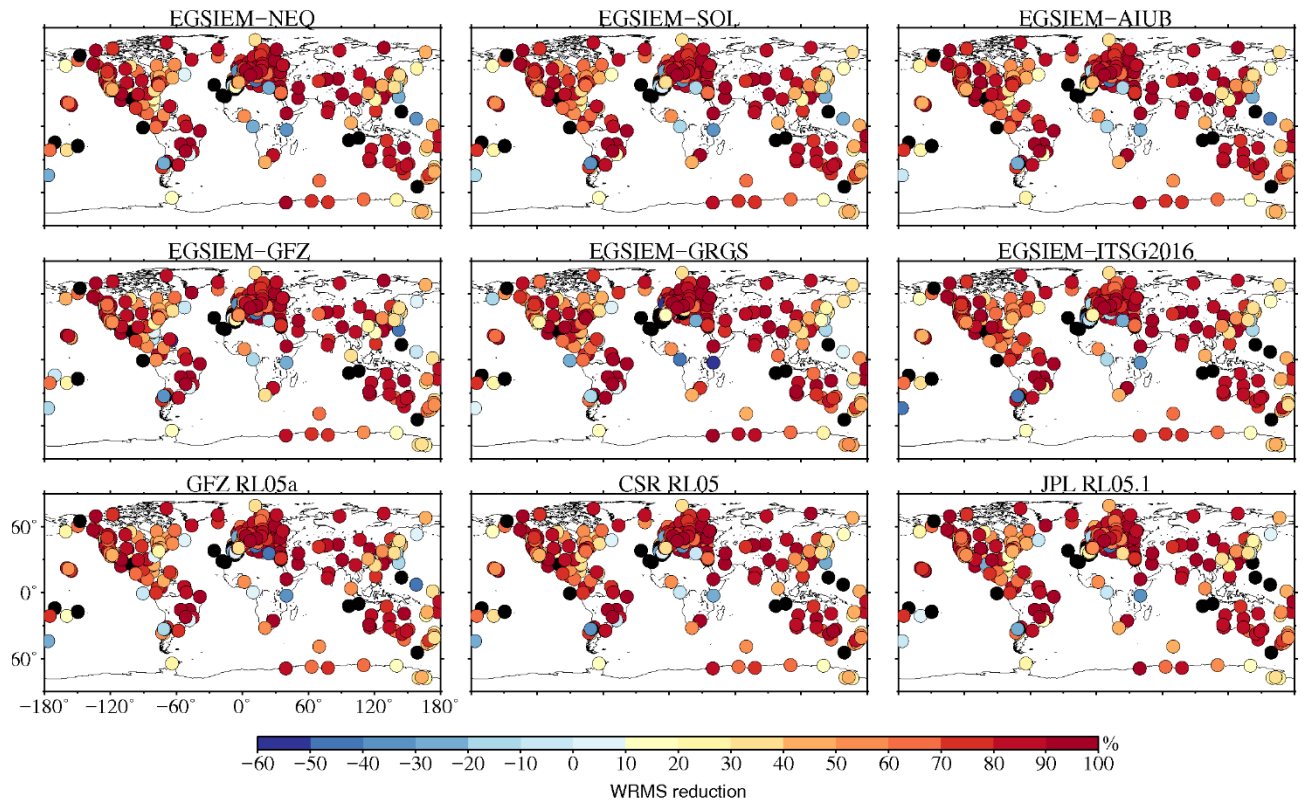


Figure 4-6: WRMS reduction at the annual signal level at 388 global GNSS stations. GRACE gravity solutions up to their full spectrum are used to compute the displacements.

In addition to the full signal and the annual signal levels, Figure 4-7 shows the mean accumulative degree WRMS reduction at the residual level after removing annual signals from both GNSS and GRACE. EGSIM-NEQ shows the best agreement with the ITRF2014 time series at the residual level as well.

Based on the validation presented above, we conclude that EGSIM-NEQ gravity solutions outperform other gravity solutions.

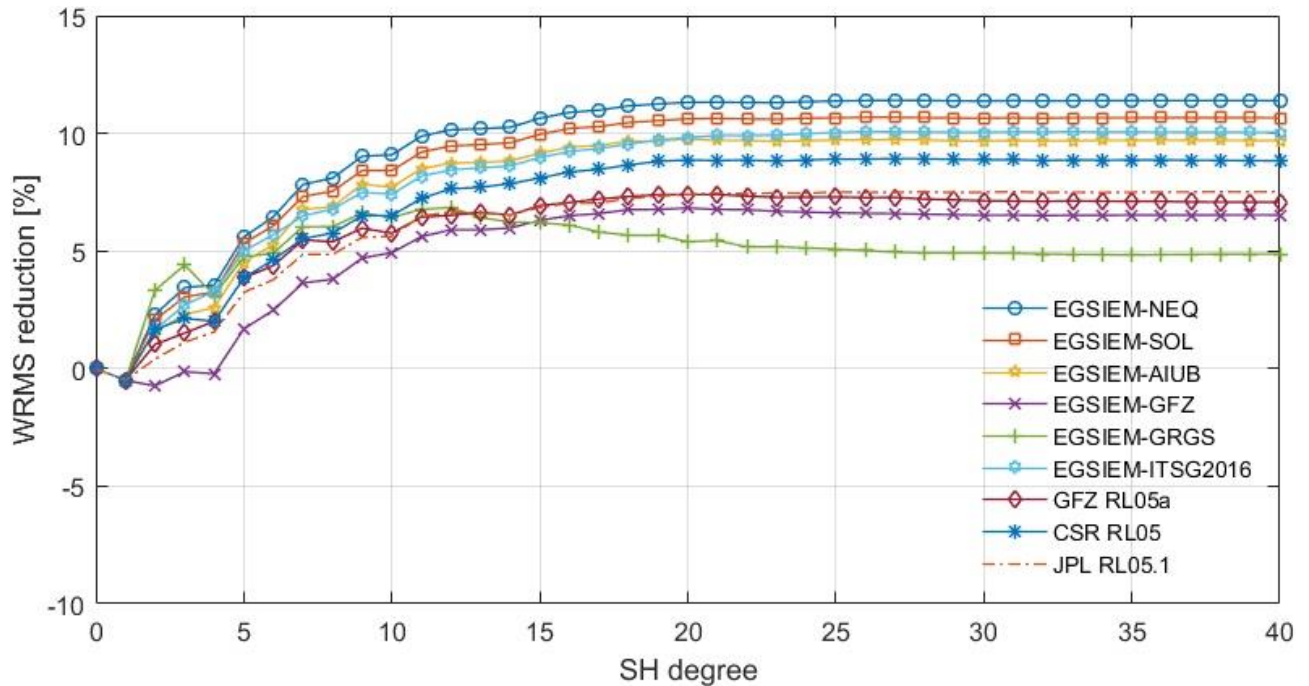


Figure 4-7: Mean accumulative degree WRMS reduction of different gravity solutions at the residual signal level up to degree 40.

4.2 Validation of EGSiem Level 3 land products

Based on EGSiem Level 2 combined solutions at the NEQ-level, EGSiem Level 3 products are generated, see details in D4.2. Table 4-3 shows the post-processing procedures to create Level 3 EWH grids for land hydrology. As reference, the procedure of GRACE Tellus to create the Level 3 land EWH grids based on their three official gravity solutions is included in Table 4-3 as well. As shown in Table 4-3, generation of the EGSiem L3 land grids are different from the GRACE Tellus land grids in terms of the C_{20} term, degree-1 SHCs as well as the selected filtering schemes.

Table 4-3 Post-processing procedure for EGSiem and GRACE Tellus to generate L3 EWH grids

	EGSIEM L3 for Land	GRACE Tellus L3 for Land
C_{20} coefficient	no replacement	replaced from SLR (Cheng et al, 2011)
Degree-1 SHCs	restored from SLR by Sośnica et al (2015)	restored from Swenson et al (2008)
GIA correction	correction applied based on the GIA model from A and Wahr (2013)	correction applied based on the GIA model from A and Wahr (2013)
Filter scheme	time-varying filters (D4.2)	destriping filter plus Gaussian filter of 300 km
GAC	not added back	not added back
EWH grids	$1^\circ \times 1^\circ$ global grids	$1^\circ \times 1^\circ$ global grids

To validate the two-year (2006&2007) EGSiem L3 land grids against the GRACE Tellus L3 land grids, we use the the same 388 ITRF2014 GNSS time series as used in Section 4.1. The Green’s functions approach is used to convert the EGSiem L3 and the GRACE Tellus L3 land grids into vertical displacements. Mean and trend for each station are fitted and removed. Note that we

remove the GAC-induced displacements beforehand in the ITRF2014 GNSS time series to make GNSS and GRACE consistent in this regard. However, due to this operation, the WRMS reduction values will be decreased compared to that presented in Section 4.1. Nevertheless, the validation process is valid to reveal the same conclusion, see Annexes for demonstration.

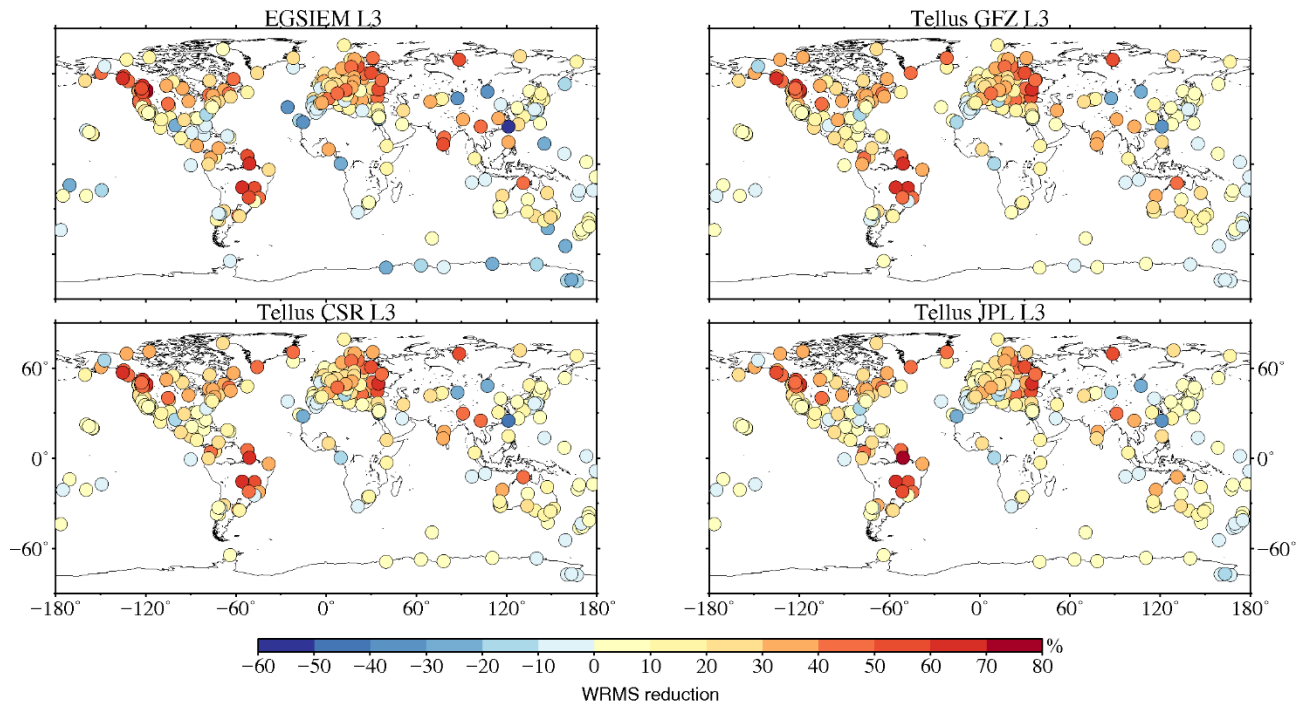


Figure 4-8: WRMS reduction at the full signal level at 388 global GNSS stations for the Level 3 grids.

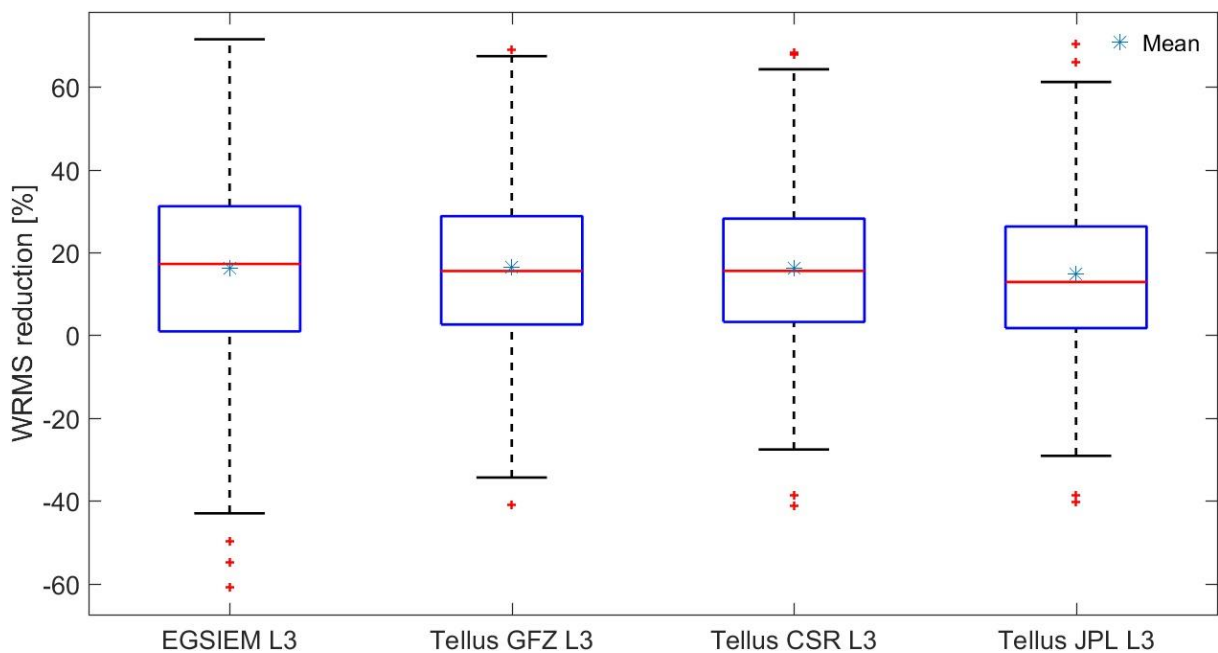


Figure 4-9: Boxplots showing WRMS reduction distributions over 388 global GNSS stations at the full signal level for the Level 3 land grids. Boxplots summarize statistics of median (red line), mean (asterisk) and the first (bottom line of the blue box) and third (top line of the blue box) quartiles.

Spatial plot in Figure 4-8 illustrates the similar patterns as shown in Figure 4-3 that most of the GNSS stations show a positive WRMS reduction. The boxplots in Figure 4-9 summarizes the statistics showing that EGSiEM L3 land grids agrees slightly better with the GNSS time series than the GRACE Tellus L3 land grids at the full signal level.

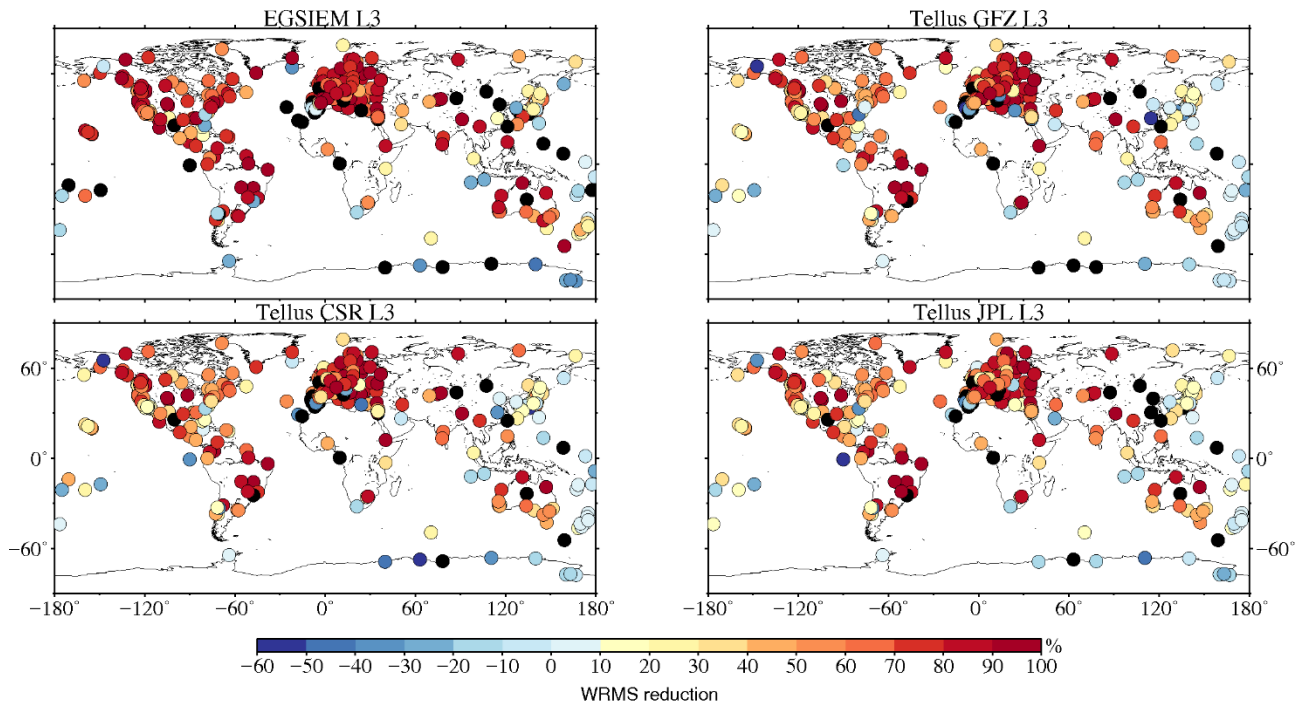


Figure 4-10: WRMS reduction at the annual signal level at 388 global GNSS stations for the Level 3 land grids.

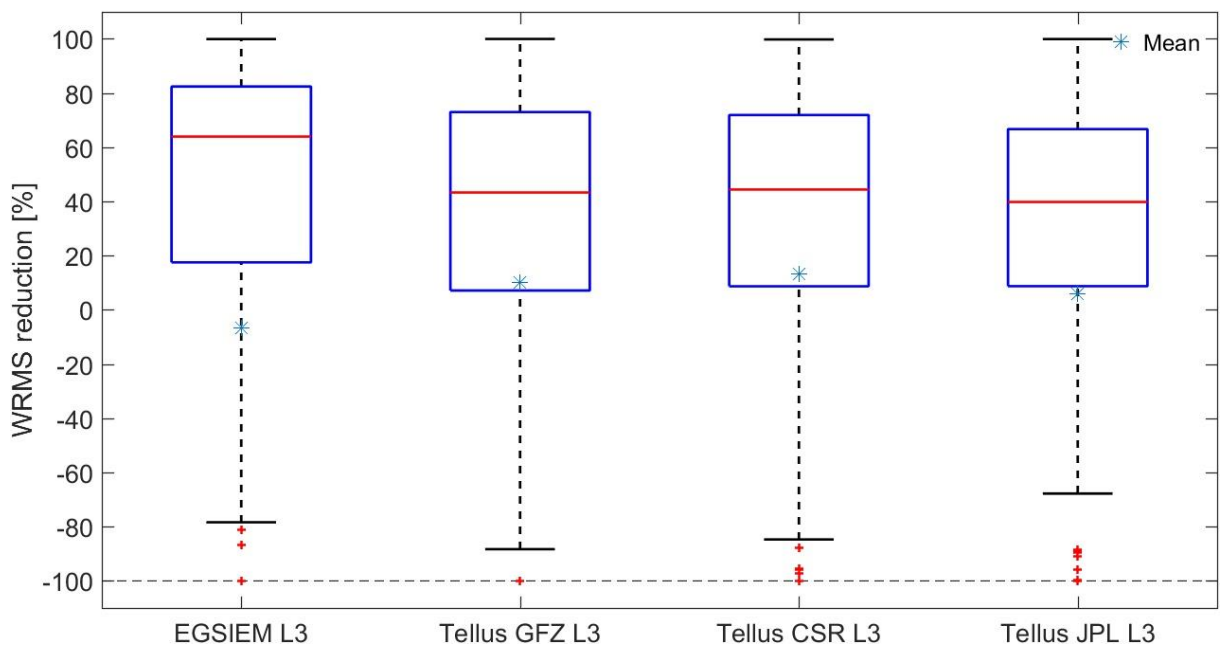


Figure 4-11: Boxplots of WRMS reductions at the annual signal level at 388 global GNSS stations for the Level 3 land grids.

Figure 4-10 displays the WRMS reduction at the annual signal level between the L3 land grids derived displacement and the ITRF2014 GNSS time series over the 388 GNSS stations. Similarly, up to nearly 100% agreements are found for all the four Level 3 products. Mean and median WRMS reductions are summarized in Figure 4-11. Mean WRMS reductions are biased by these extreme negative WRMS reductions. In terms of the quartiles, EGSIM L3 products clearly outperform other three GRACE Tellus Level 3 land products at the annual signal level.

According to the validation using the ITRF2014 residuals for the L3 grids, we conclude that the EGSIM L3 land grids show better performances than the L3 land grids from the GRACE Tellus.

5. Validation based on OBP

To objectively assess the differences between GRACE solutions, it is necessary to validate them against independent observations. Ocean bottom pressure data from a set of globally distributed sensors can be directly compared with the gravity field solutions, and therefore can be used for their validation. After pre-processing the in situ data, relative explained variance, i.e. the variance of the in situ data explained by the model, is calculated for every OBP station with available data.

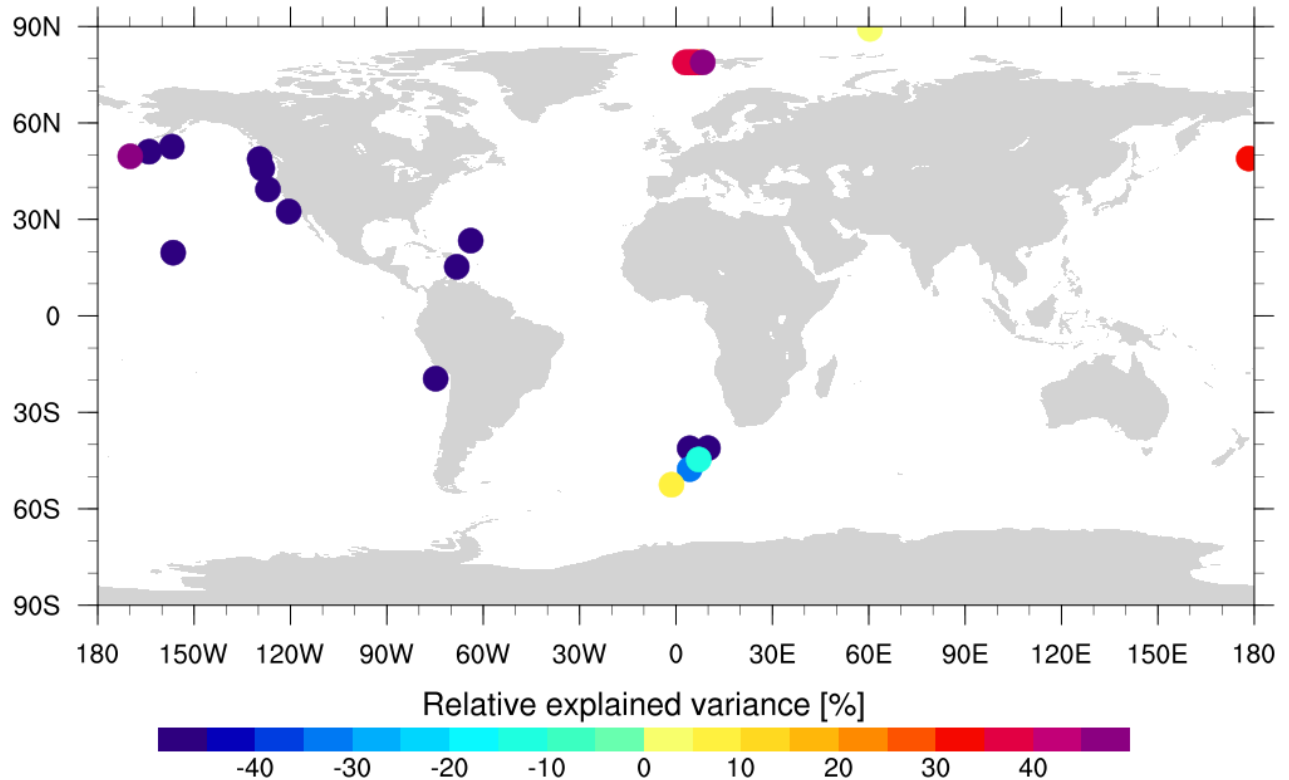


Figure 5-1: Relative explained variance (%) for the EGSIM Level 3 ocean product for years 2006-2007

The validation procedure is applied to the EGSIM Level 3 ocean product for the ocean for years 2006 and 2007 (Figure 5-1). For comparison, the three official Tellus solutions from CSR, GFZ and JPL for the same years (Figure 5-2 left), as well as for the whole available time span, 2002-2016 (Figure 5-2 right), are also validated by using the same procedure. While there are 105 in situ stations with data in the whole time span, in the two years for which the EGSIM Level 3 ocean product was available only 24 station had sufficiently long time series. The EGSIM L3 ocean product displays relatively good agreement with the in situ data in the Polar Regions, with relative explained variance up to 45%, but poor agreement in the lower latitudes, where the relative explained variance is negative for most station. In comparison, the Tellus solutions for the same two year time span show a slightly better agreement with the in situ data than the EGSIM Level 3 ocean product, but for them too there are only a few stations with positive relative explained variance. On the other hand, when validating longer time series the results are considerably better, with more stations with positive explained variance and better global coverage. That, as well as the low total number of stations with data available in that two year time span, suggests that a two year

long time series of GRACE gravity fields is not long enough for obtaining conclusive results from the validation with in situ OBP.

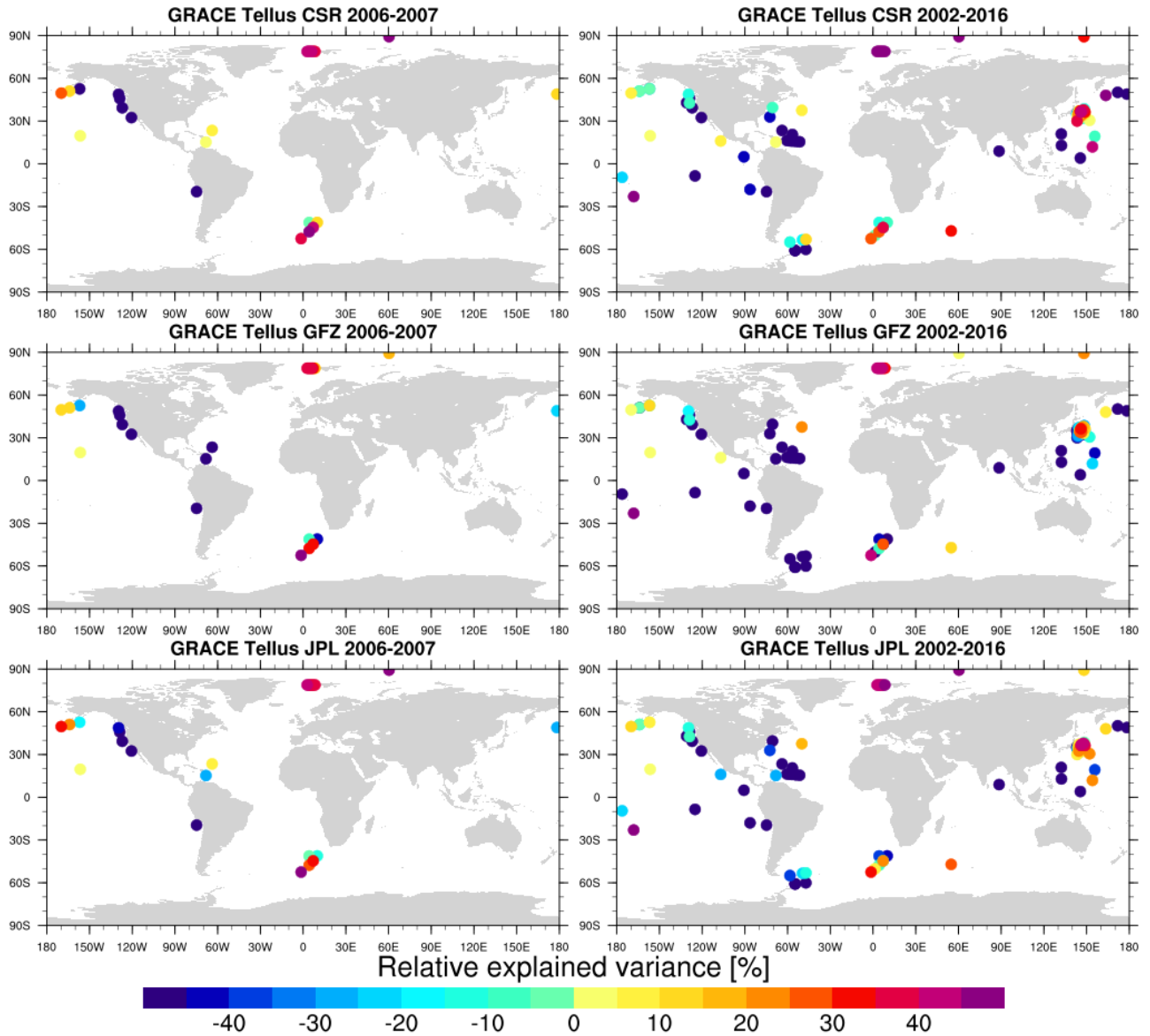


Figure 5-2: Relative explained variance (%) for CSR, GFZ and JPL Tellus solutions for years 2006-2007 (left) and for years 2002-2016 (right).

6. Error budgeting

During the internal validation of the gravity solutions from ACs and the combined solutions in D4.2, intensive error/noise analysis has been done in the spectral domain as well as in the spatial domain in terms of equivalent water height. In D4.2, anomalies are regarded as the residuals with respect to a deterministic model of time-variations of a single gravity solution itself. Alternatively, in this section we continue the error budgeting analysis by assessing the differences between the two EGSIEM combined solutions, which is defined as:

$$\text{EGSIEM-NEQ} - \text{EGSIEM-SOL}$$

and represented in terms of SHCs as

$$\begin{aligned} \sigma_{lm}^C &= C_{lm}^{\text{EGSIEM-NEQ}} - C_{lm}^{\text{EGSIEM-SOL}}, \\ \sigma_{lm}^S &= S_{lm}^{\text{EGSIEM-NEQ}} - S_{lm}^{\text{EGSIEM-SOL}}. \end{aligned}$$

We assume that the geophysically meaningful signals are removed by differencing and the remaining residuals are considered as errors. We assess the magnitude of the errors by mapping them into the spatial domain in terms of displacements into $1^\circ \times 1^\circ$ grids globally. RMS values are calculated for each grid accordingly based on the two-year data (2006&2007).

Figure 6-1 displays the differences of the unitless spherical harmonic coefficients between EGSIEM-NEQ and EGSIEM SOL in January 2006. Clearly, most of differences are represented in the high degree/order SHCs.

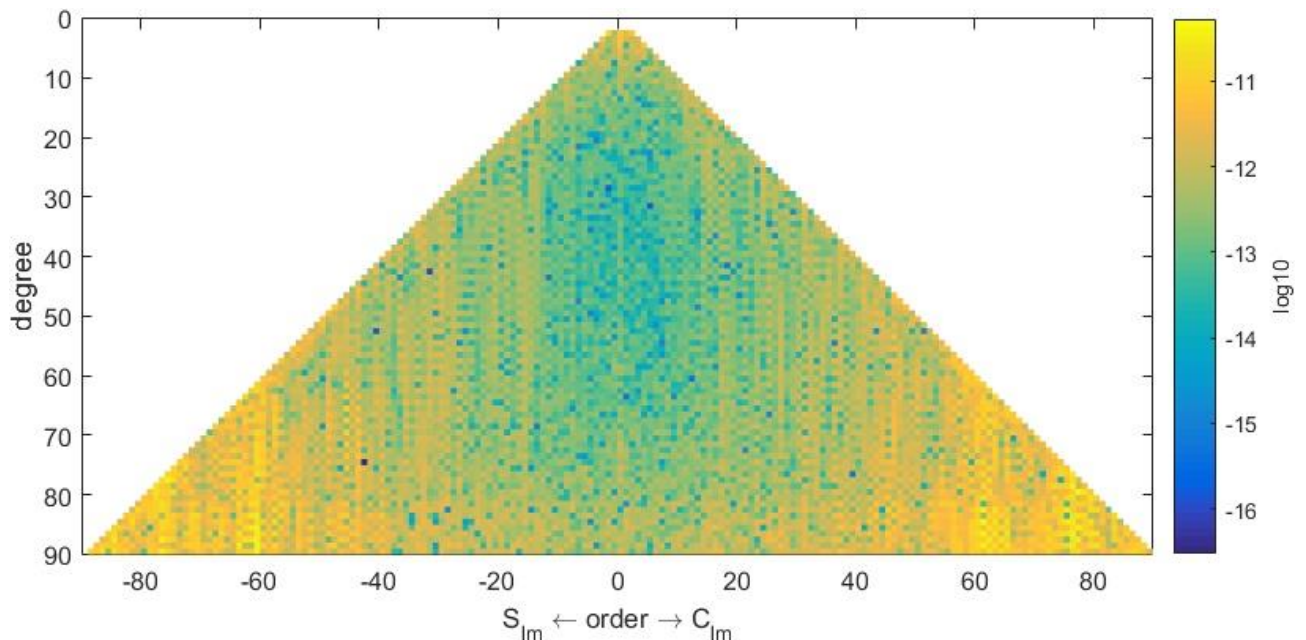


Figure 6-1: Differences of SHCs between EGSIEM-NEQ and EGSIEM-SOL in January 2006.

Spatial error representation in terms of displacements

We map the differences into the spatial domain in terms of displacements by the spherical harmonic approach. Figure 6-2 to 6-4 represents the mapped displacements in the North, East and Vertical components without applying any filtering. Obviously, north-south strips dominate the spatial

patterns of all three components which is due to the orbital configuration of the GRACE satellites. The biggest RMS value of the errors is seen in the vertical component up to 17 mm. Smaller RMS values are observed in the North and East components with maximum RMS values up to 1.2 mm and 5 mm, respectively.

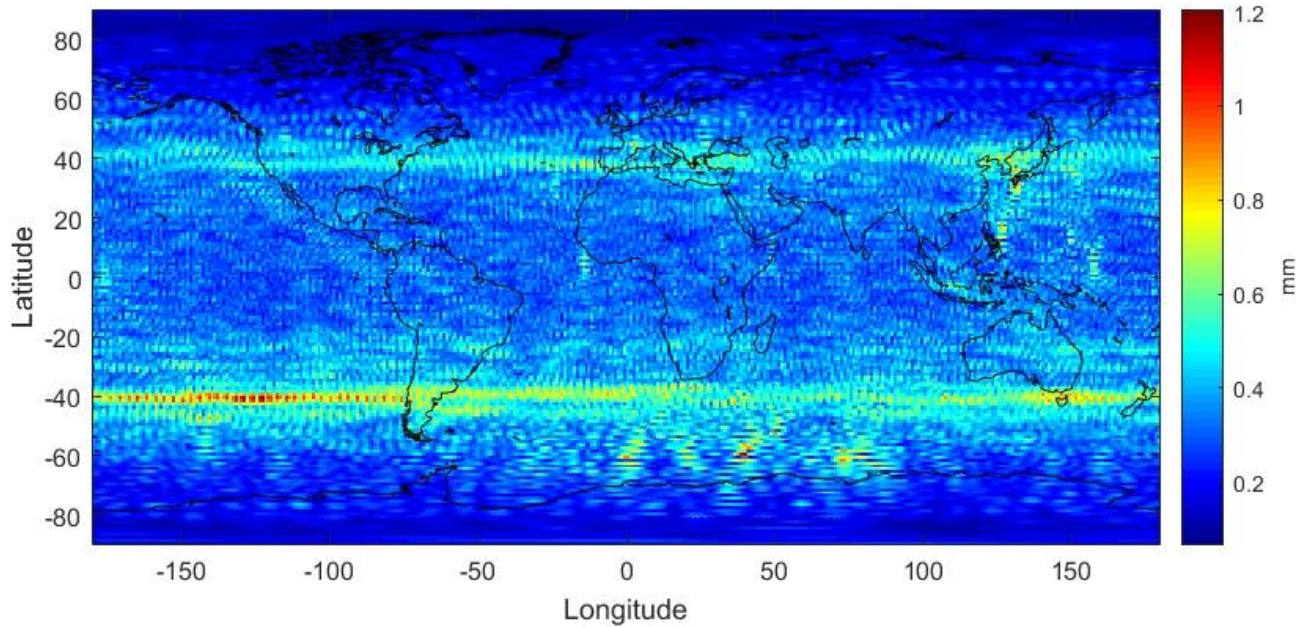


Figure 6-2: RMS of mapped errors into displacements in the North component. No filter is applied.

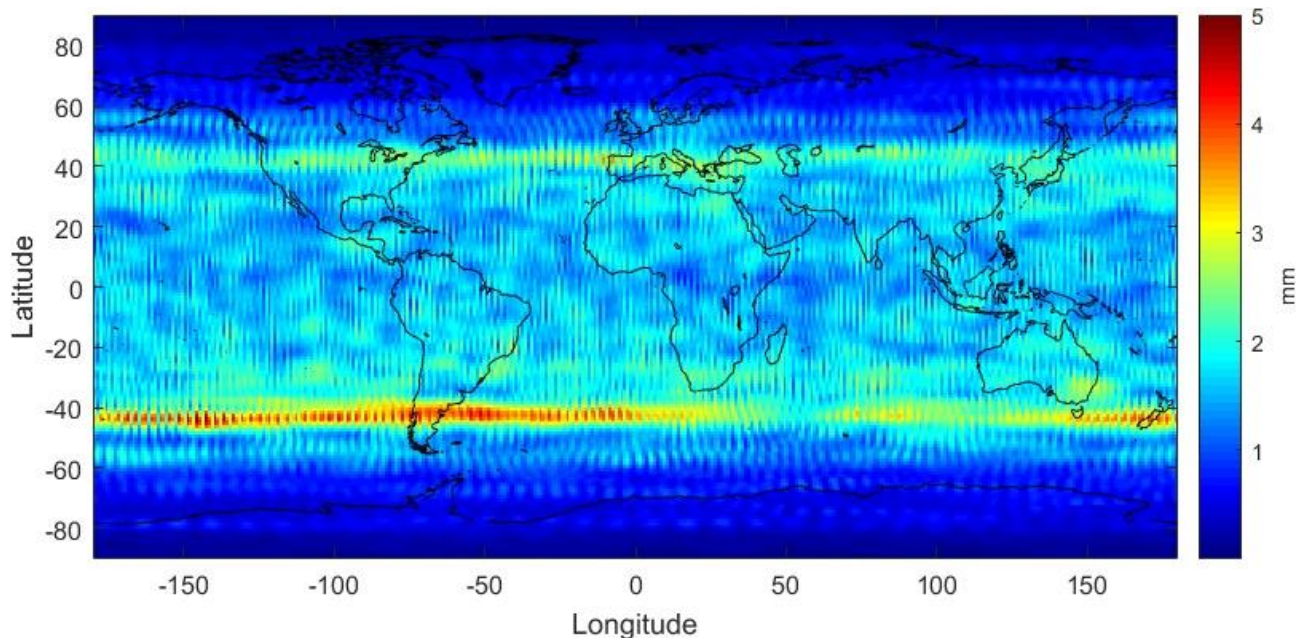


Figure 6-3: RMS of mapped errors into displacements in the East component. No filter is applied.

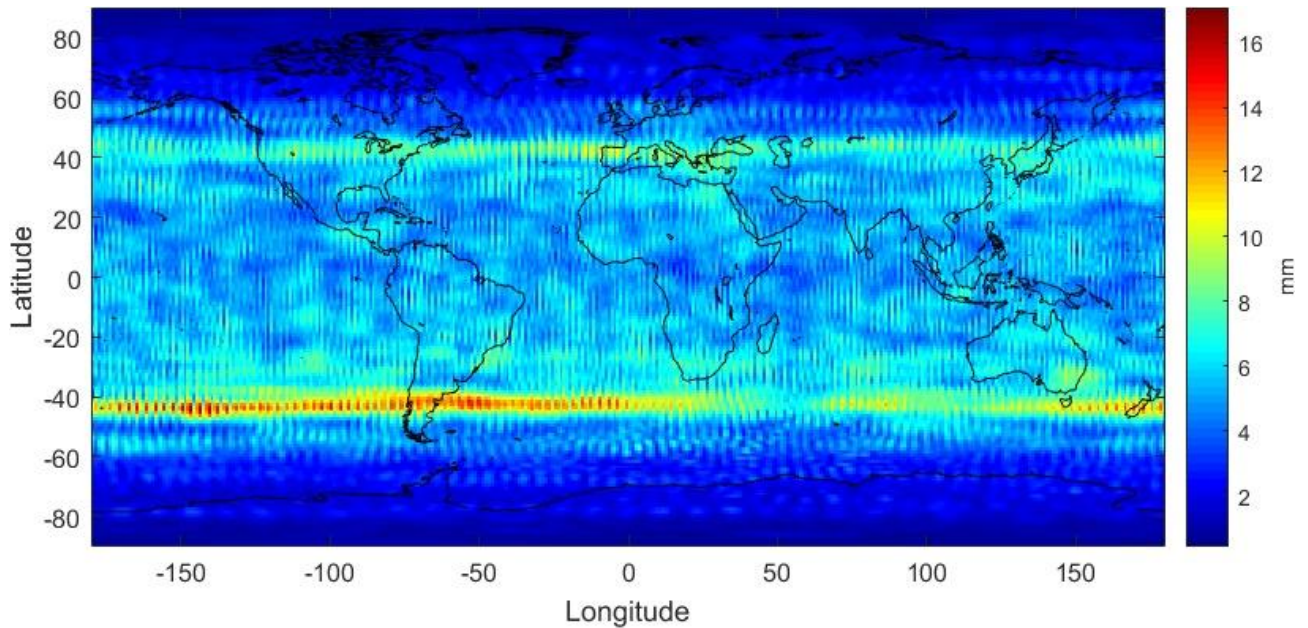


Figure 6-4: RMS of mapped errors into displacements in the Vertical component. No filter is applied.

Figure 6-5 to 6-7 illustrate the RMS of mapped displacements after a moderate Gaussian filter of 500 km is applied. This choice of filter is commonly used when we compare the GRACE-derived displacements with GPS-observed counterparts. After smoothing, RMS values are significantly reduced in all the three components down to maximum 0.06 mm, 0.06 mm and 0.8 mm, respectively.

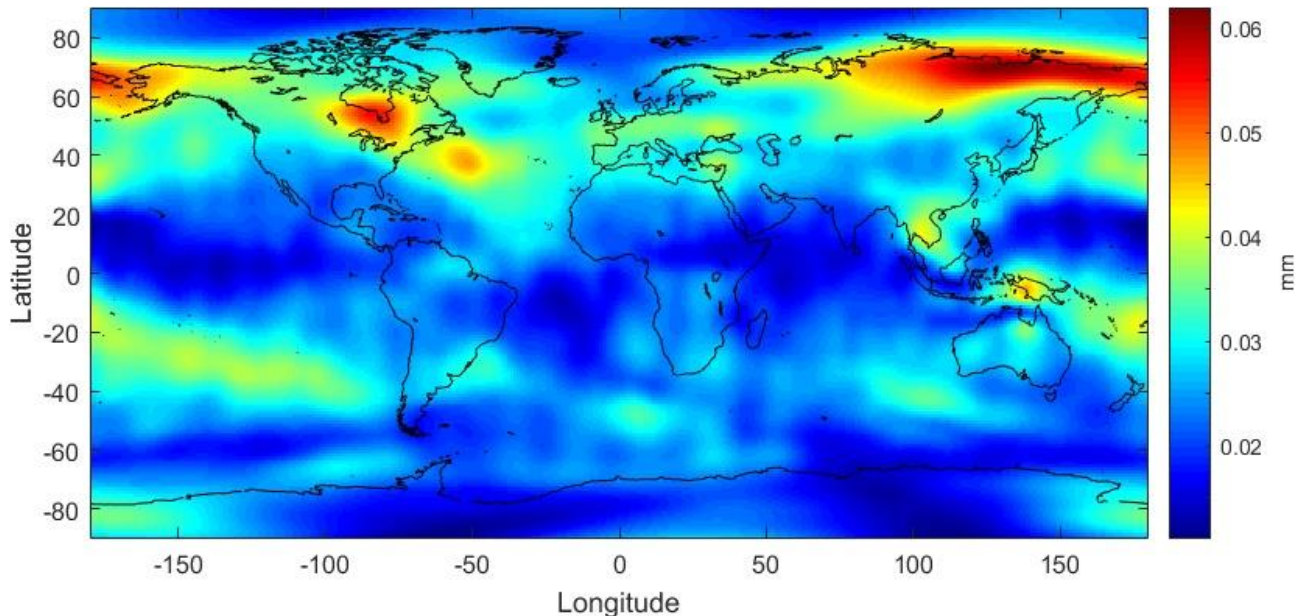


Figure 6-5: RMS of mapped errors into displacements in the North component. A moderate Gaussian filtering of 500 km is applied.

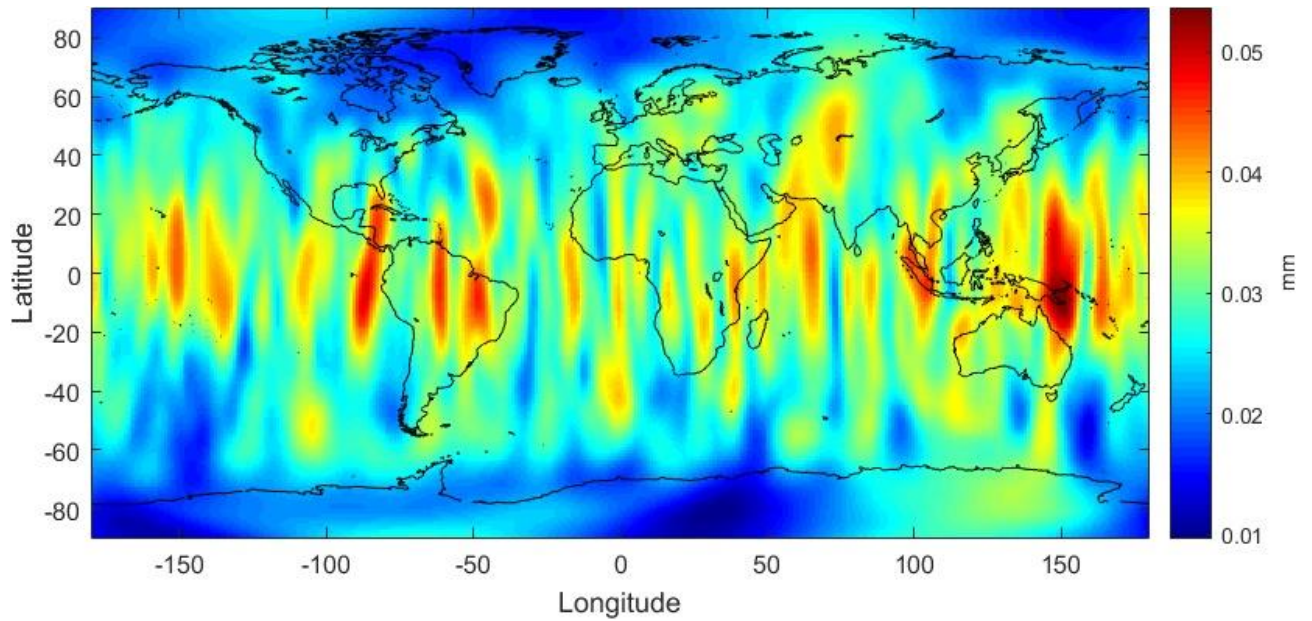


Figure 6-6: RMS of mapped errors into displacements in the East component. A moderate Gaussian filtering of 500 km is applied.

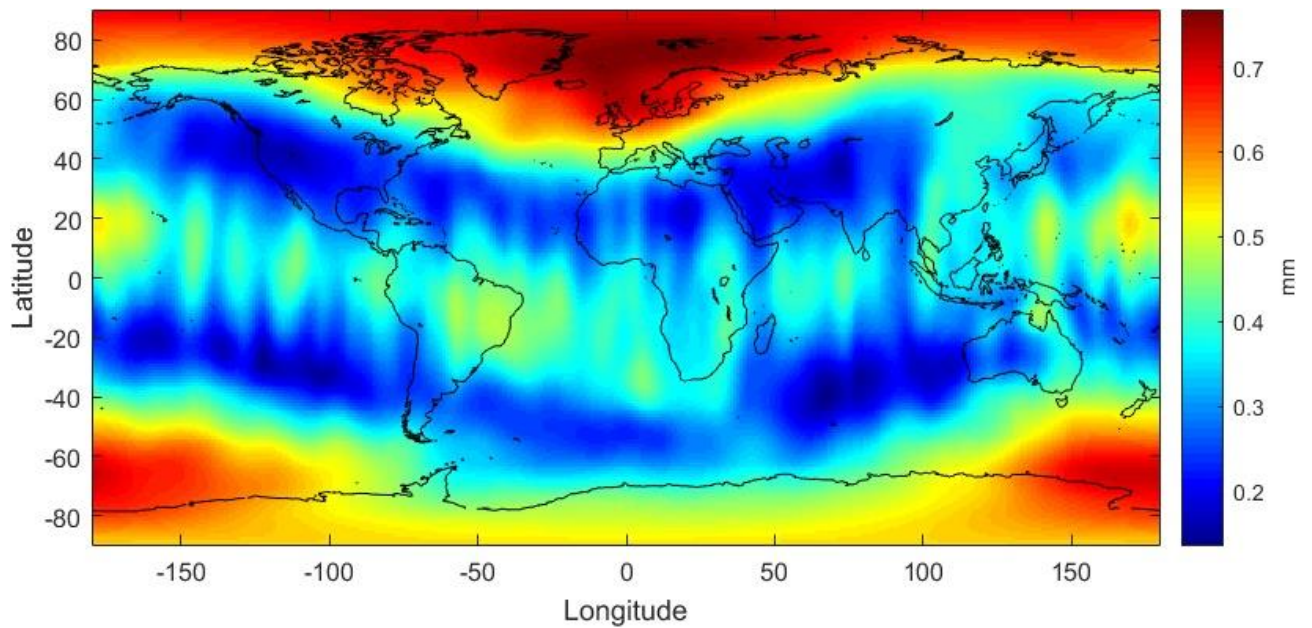


Figure 6-7: RMS of mapped errors into displacements in the Vertical component. A moderate Gaussian filtering of 500 km is applied.

7. Bibliography

A G., J. Wahr, S. Zhong, 2013: Computations of the viscoelastic response of a 3-D compressible Earth to surface loading: an application to Glacial Isostatic Adjustment in Antarctica and Canada. *Geophys. J. Int.*, vol(192), pp. 557–572, doi: 10.1093/gji/ggs030

Cheng M., J. C. Ries, B. D. Tapley, 2011: Variations of the Earth's figure axis from satellite laser ranging and GRACE. *J. Geophys. Res.*, vol(116), B01409, doi: 10.1029/2010JB000850.

van Dam T., J. Wahr, D. Lavallée, 2007: A comparison of annual vertical crustal displacements from GPS and Gravity Recovery and Climate Experiment (GRACE) over Europe. *J. Geophys. Res.*, vol (112), B03404, doi: 10.1029/2006JB004335

Gu Y., D. Fan, W. You, 2017: Comparison of observed and modeled seasonal crustal vertical displacements derived from multi-institution GPS and GRACE solutions. *Geophys. Res. Lett.*, 44, 7219–7227, doi: 10.1002/2017GL074264.

Rebischung P., Z. Altamimi, J. Ray, G. Bruno, 2016. *Journal of Geodesy*, vol(90): 611, doi: 10.1007/s00190-016-0897-6

Sośnica K., A. Jäggi, U. Meyer, D. Thaller, G. Beutler, D. Arnold, R. Dach, 2015: Time variable Earth's gravity field from SLR satellites. *Journal of Geodesy*, vol. 89(10), pp. 945-960, doi: 10.1007/s00190-015-0825-1.

Swenson S.C., D. P. Chambers, J. Wahr, 2008: Estimating geocenter variations from a combination of GRACE and ocean model output. *J Geophys. Res.-Solid Earth*, vol(113), B08410, doi:10.1029/2007JB005338.



8. Glossary

AC	Analysis Center
AIUB	Astronomical Institute, University of Bern
CSR	Center for Space Research, Austin, Texas
EGSIEM	European Gravity Service for Improved Emergency Management
EWH	Equivalent Water Height
GAC	Geopotential coefficients of averaged combination of non-tidal atmosphere and ocean
GFZ	Helmholtz Centre Potsdam, German Research Centre for Geosciences
GNSS	Global Navigation Satellite System
GRACE	Gravity Recovery and Climate Experiment
GRGS	Groupe de Recherche de Géodésie Spatiale, Toulouse, France
GSM	Geophoten coefficients of GRACE-derived static gravity field
ICGEM	International Center for Global Earth Models
ITRF	International Terrestrial Reference Frame
JPL	Jet Propulsion Laboratory, Pasadena, California, USA
NEQ	Normal Equation
OBP	Ocean Bottom Pressure
RMS	Root Mean Square
SDS	Science Data System
SHC	Spherical Harmonic Coefficient
SLR	Satellite Laser Ranging
VCE	Variance Component Estimation
WRMS	Weighted RMS

9. Annexes

WRMS reduction and its variants

WRMS reduction is used commonly to evaluate the agreements between GNSS-observed and GRACE-derived displacements, see van Dam et al. (2007), which is defined as

$$\text{WRMS reduction} = \frac{\text{WRMS}[\text{GPS}] - \text{WRMS}[\text{GPS} - \text{GRACE}]}{\text{WRMS}[\text{GPS}]} = 1 - \frac{\text{WRMS}[\text{GPS} - \text{GRACE}]}{\text{WRMS}[\text{GPS}]}$$

It represents the percentage of signals in the GNSS time series which can be explained by GRACE and it ranges from minus infinity to 1, i.e. 100%. It should be mentioned that the terminology relative explained variance used in Section 5 is equivalent to the terminology WRMS reduction used in Section 4. Its variant degree WRMS reduction is accordingly defined as

$$\text{Degree WRMS reduction} = 1 - \frac{\text{WRMS}[\text{GPS} - \text{GRACE}^n]}{\text{WRMS}[\text{GPS}]}$$

Superscript n indicates that the SHCs at degree n only from GRACE are used to compute the displacements. Certainly, we can use the SHCs up to degree n to indicate the accumulative degree WRMS reduction.

Figure 9-1 is to demonstrate that the WRMS reduction values will be lowered when GAC-induced displacements are removed in the GNSS time series. Compared to Figure 4-2 which is produced when GAC products are added back to GRACE, the mean accumulative degree WRMS reduction is lowered by roughly 10%. This is reasonable as the denominator $\text{WRMS}[\text{GPS}]$ is decreased by removing the GAC-derived displacements, see the formular above. Nevertheless, the same conclusion can be reached in both Figure 4-2 and Figure 9-1.

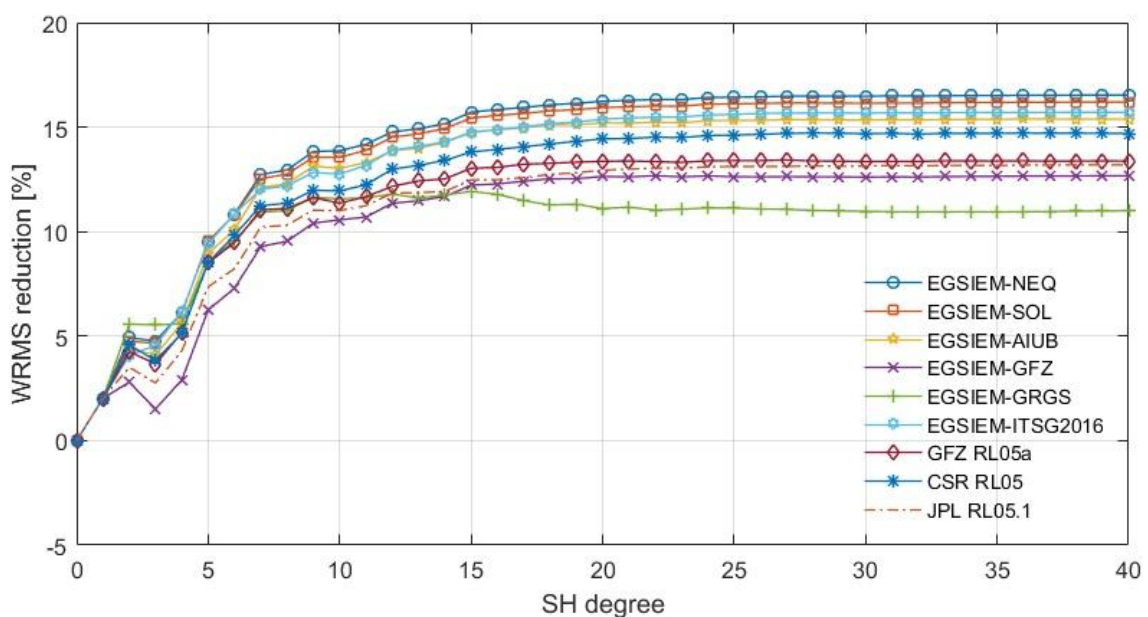


Figure 9-1: Mean accumulative degree WRMS reduction of different solutions at the full signal level up to degree 40. Note that GAC-induced displacements are removed in the GNSS time series.